HHS Public Access

Author manuscript

Biol Psychiatry Cogn Neurosci Neuroimaging. Author manuscript; available in PMC 2021 November 01.

Published in final edited form as:

Biol Psychiatry Cogn Neurosci Neuroimaging. 2020 November ; 5(11): 1011–1018. doi:10.1016/j.bpsc.2020.07.006.

Temporal dynamics of large-scale networks predict neural cue reactivity and cue-induced craving

Kainan S. Wang, Ph.D.[1,2], **Roselinde H. Kaiser, Ph.D.**[3], **Alyssa L. Peechatka, Ph.D.**[1,2], **Blaise B. Frederick, Ph.D.**[1,2], **Amy C. Janes, Ph.D.**[1,2]

[1]McLean Imaging Center, McLean Hospital, Belmont, MA, USA

[2]Harvard Medical School, Boston, MA, USA

[3]Department of Psychology and Neuroscience, University of Colorado, Boulder, CO, USA

Abstract

Background—Cue reactivity, a core characteristic of substance used disorders, commonly recruits brain regions that are key nodes in neurocognitive networks including the default mode network (DMN) and salience network (SN). Whether resting-state temporal dynamic properties of these networks relate to subsequent cue reactivity and cue-induced craving is unknown.

Methods—The resting-state data of 46 nicotine-dependent participants were assessed to define temporal dynamic properties of DMN and SN states. Temporal dynamics focused on the total time across the scan session that brain activity resides in these specific states. Using regression models, we examined how the total time in each state related to neural reactivity to smoking cues within key DMN (posterior cingulate cortex, medial prefrontal cortex) or SN nodes (anterior insula [AI], dorsal anterior cingulate cortex [dACC]). Mediation analyses were subsequently conducted to study how neural cue reactivity mediates the relationship between total time in state at rest and subjective cue-induced craving.

Results—Increased time spent in the DMN state and decreased time spent in the SN state predicted subsequent cue-induced increases in the AI and dACC, respectively. Cue-induced AI and dACC activity significantly mediated the relationship between time spent in DMN/SN and cue-induced subjective craving.

Conclusions—Our findings showed a significant relationship between resting-state dynamics of the DMN/SN and task-activated SN nodes that together predicted cue-induced craving changes in nicotine-dependent individuals. These findings propose a neurobiological pathway for cue-induced craving that begins with resting-state temporal dynamics, suggesting that brain responding to external stimuli is driven by resting temporal dynamics.

Address for correspondence: Kainan S. Wang, Ph.D., MIC Mail Stop 319, 115 Mill St., McLean Hospital/Harvard Medical School, Belmont, MA, 02478, kwang23@mclean.harvard.edu, Phone: (617) 855-2419.

Conflict of Interest:
The authors report no biomedical financial interests or potential conflicts of interest.

Keywords

temporal dynamics; default mode network; salience network; cue reactivity; craving; substance use disorder

Introduction

Heightened reactivity towards drug-related cues is a core feature of substance use disorders (SUDs; 1, 2) that often predicts future relapse (3–6). Evidence from functional magnetic resonance imaging (fMRI) studies have clarified the neurobiological underpinnings of cue reactivity by showing that brain regions such as the anterior insula (AI), dorsal anterior cingulate cortex (dACC), medial prefrontal cortex (mPFC), and posterior cingulate cortex (PCC) commonly react to drug-related cues (7). Cue-induced activation of these brain regions has been linked to subjective and behavioral aspects of addiction, such as a rise in subjective craving (8) and heightened relapse vulnerability (4, 9, 10). Beyond addiction, these regions are primary nodes of two neurocognitive networks, the default mode network (DMN; mPFC and PCC) and the salience network (SN; insula and dACC), which play fundamental roles in internally-directed cognition and salience processing respectively (11–13). It is plausible that drug cues not only lead to the activation of the DMN and SN, but that the inherent function of these networks, even without cue exposure, impacts one's vulnerability to be cue reactive. As such, there might be a neural pathway linking how the brain functions at rest with its subsequent reactivity during cue exposure that collectively drives cue-induced changes in subjective craving.

Within the field of addiction, the DMN and SN have typically been assessed during task-free resting-state scans using static connectivity measures (for review see 14) that quantify correlated brain activity over extended time periods (15). Variance in DMN and SN static connectivity relate to both the susceptibility and maintenance of addictive behavior (16). For instance, in drug-naive rats, enhanced resting static connectivity between the insula and striatum predicts increased likelihood of developing physiological withdrawal, which contributes to nicotine dependence (17). Moreover, heightened functional connectivity between the DMN and SN is related to greater abstinence-induced subjective craving (18). However, static connectivity does not consider the time-varying or dynamic patterns of these networks (19). Few studies have investigated the temporal dynamics of resting-state networks in SUDs but one showed that dynamic resting-state connectivity between the DMN/SN and insular subregions was reduced during nicotine abstinence compared to satiety (20). As such, evaluating temporal dynamics promises to bolster our understanding of how resting-state network function influences core elements of addiction including cue reactivity, and will substantiate the applicability of using resting-state networks as biomarkers to predict cue-induced subjective craving, which drives relapse vulnerability.

To address this gap, we evaluated nicotine-dependent participants using fMRI and collected data first at rest and then during a smoking cue-reactivity task. For the resting-state data, we applied a novel co-activation pattern analysis, which we used previously in a sample of healthy individuals (N = 462) to parcellate the brain into distinct networks-of-interest

including the DMN and SN (21). We applied these previously-identified states to calculate the total time spent in the DMN and SN across the entire resting timeseries. We then used a staged analysis approach to test the overarching hypothesis that DMN/SN resting-state dynamics impact cue reactivity. We first studied whether DMN/SN resting-state dynamics predicted DMN/SN nodal cue reactivity and informed by the results, we subsequently conducted a mediation analysis to study how cue reactivity influenced the link between resting-state dynamics and cue induced craving. Collectively, this work aimed to show that resting temporal dynamics is part of the neurobiological pathway preceding cue reactivity and craving.

Methods and Materials

Participants

Forty-six (19 females) nicotine-dependent participants (Table 1) were recruited as part of a larger study. This current sample partially overlapped with a previously published manuscript that did not evaluate temporal dynamics (22). At time of screening, participants had a Fagerstrom Test for Nicotine Dependence (23) score ≥ 4 (mean score: 5.59 +/− 1.59), an expired carbon monoxide concentration ≥ 5 ppm (mean: 22.24 +/− 12.44), tested negative for pregnancy via urinalysis, and had no report of serious medical illness. Participants were administered the structured clinical interview for DSM-IV-TR (24) to screen them for drug or alcohol dependence (except nicotine), major depressive disorder within the past three months, and lifetime history or current diagnosis of any of the following psychiatric illnesses: schizophrenia, schizoaffective disorder, delusional disorder, psychotic disorders not otherwise specified, bipolar disorder, and mood congruent or incongruent psychotic features. Abstinence from drug and alcohol use was confirmed by urine and breath samples, respectively (QuickTox11 Panel Drug Test Card; Branan Medical Corporation, Irvine, CA; Alco-Sensor IV; Intoximeters, St. Louis, MO). Participants provided written informed consent in accordance with the experimental protocol approved by the Partners HealthCare Institutional Review Board upon receiving a complete description of the experiment.

Experimental setup

As in our prior work (1, 22), participants were asked to maintain their typical smoking habits prior to the study visit. To normalize all procedures relative to the last cigarette smoked, participants smoked one of their own cigarettes in the laboratory approximately one hour before entering the fMRI scanner. Fifteen minutes before scanning, participants completed the Questionnaire of Smoking Urges (QSU; 25) as a subjective evaluation of their pre-cue exposure craving. In the scanner, participants first completed a 6-minute resting-state scan where they were presented with a blank black screen and given the instruction to keep their eyes open and think of nothing in particular. Participants subsequently performed the smoking cue-reactivity task. Upon exiting the scanner, participants again completed the QSU to assess their post-cue exposure craving. The total QSU score was used to separately calculate pre- and post-cue exposure craving measures. The total post minus total pre score was then computed to determine cue-induced changes in subjective craving.

Neuroimaging data collection and preprocessing

Images were collected using a Siemens Prisma 3T scanner (Siemens, Erlangen, Germany) with a 64-channel head coil. Slices for all functional images (resting state and cue-reactivity task) were acquired with the following parameters (repetition time (TR) = 720 ms; echo time (TE) = 30 ms; slices = 66; phase encode direction posterior to anterior; flip angle = 66°; voxel size = 2.5 × 2.5 × 2 × 5 mm; generalized autocalibrating partially parallel acquisitions (GRAPPA) factor of 2; and a multiband acceleration factor = 6). Following functional images, multiecho multi-planar rapidly acquired gradient echo-structural images (MPRAGE) were acquired with the following parameters (TR = 2530 ms; TE= 3.3, 6.98, 8.79, and 10.65 ms; flip angle = 7°; resolution = 1.33 × 1 × 1 mm).

Images were processed using fMRI of the Brain (FMRIB) Software Library (FSL; www.fmri-b.ox.ac.uk/fsl). All functional images were preprocessed with the same pipeline: brain extraction via BET, motion correction using MCFLIRT, coregistration and normalization to Montreal Neurological Institute (MNI) space, slice-time correction, spatial smoothing at full-width half-maximum of 6mm, and high-pass filtering at 0.01 Hz. To further address motion, prior to pre-processing we used Spikefix (https://github.com/bbfrederick/spikefix) to identify timepoints representing motion and intensity artifacts. For task data, these data spikes were removed and single point regressors representing the spike time points were added to the general linear model (GLM) as confound regressors.

Resting-state data were denoised using independent component analysis with the FSL tool for multivariate exploratory linear optimized decomposition into independent components (MELODIC). We ran MELODIC for each participant and visually inspected the spatial and temporal readout for each independent component to identify and remove noise-related components. This approach generated a denoised resting-state fMRI time series (26, 27).

Resting-state coactivation pattern analysis

The analysis is described in more details in a published manuscript (21) and further descriptions are provided in the supplementary material of this study. Briefly, we applied the maps of the DMN and SN coactivation patterns (CAPs) or “states” derived from a sample of 462 individuals from the Human Connectome Project (HCP) in (21). The DMN state (Supplementary Fig. 1), which includes the mPFC, PCC, and precuneous, overlaps with the canonical DMN (28). Likewise, the SN state (Supplementary Fig. 1), which includes the insula and dACC, overlaps with the canonical SN (29). By applying the DMN and SN states defined in the HCP sample, we were able to examine the dynamic properties of these networks in our current sample. These states were used to compute state-specific dynamic measure including the total time spent (in seconds) in each state. The total time in state can be further divided into two additional state metrics 1) frequency of transitions into each state and 2) “persistence” (i.e., average time spent in a state during each entry), both of which were evaluated and presented in the supplementary materials for completeness.

Smoking cue-reactivity task

The task was similar to that reported in our previous work (1, 22). Participants were shown 10 smoking, 10 non-smoking and 2 target images in a pseudo-random order during each of

the five runs. Smoking images contained cigarette-related content (e.g. people smoking cigarettes). Non-smoking images were matched in content with the smoking images and contained people, hands, or objects. Target images showcased animals and were included to verify attention via a button press. Images were presented for 4 seconds, followed by a jittered intertrial interval (6-14 seconds; mean: 10 seconds).

Run-level GLMs included regressors for each image type convolved with the standard gamma hemodynamic response function, confound regressors for motion timecourses (x, y, and z translation and rotation) and the artifacts defined by Spikefix. Participant-level GLMs were modeled by averaging each participant's five runs in a fixed-effects model. Regions-of-interest (ROI)-specific parameter estimates for smoking – non-smoking contrast were extracted for each participant.

We defined two sets of *a priori* ROIs based on: 1) their roles in either the DMN or SN, and 2) meta-analytic results showing that these regions commonly respond to smoking cues (7). Using ROIs from prior work, we defined three DMN nodes (11): the posterior cingulate cortex (PCC; 30) and medial prefrontal areas including the ventromedial prefrontal cortex (vmPFC; 31) and rostral anterior cingulate cortex (rACC; 32) and two nodes of the SN: the dorsal anterior cingulate cortex (dACC; 1) and bilateral anterior insula (AI; 33). In a follow-up analysis, the bilateral AI was parcellated into four anatomically-defined subregions: 1) anterior short gyrus, 2) middle short gyrus, 3) posterior short gyrus and 4) the anterior pole (33). All ROIs are presented in supplementary figure 2.

Data Analysis

We conducted staged analyses to determine links between resting-state dynamics and cue reactivity. First, we used multivariate multiple regression models to evaluate whether DMN and SN resting dynamics together predicted cue reactivity in either DMN (PCC, vmPFC, and rACC) or SN (AI and dACC) ROIs. We applied Bonferroni correction on the two regression models with the adjusted α threshold of $0.05/2 = 0.025$. Informed by these findings, we determined whether cue-induced activation mediated the relationship between resting-state dynamics and cue-induced rise in subjective craving. Finally, on an exploratory level, we parcellated the AI into its anatomic subregions to further refine the pathway leading to cue-induced craving. This staged analysis did not require a correction for multiple comparisons across levels as these complementary analyses collectively tested the overarching hypothesis that resting-state dynamics drive cue reactivity and cue-induced craving. These analyses together permitted us to define a neurobiological path originating from resting dynamics to changes in cue-induced subjective craving. All mediation analyses were carried out using PROCESS (v. 3.3; 34) in SPSS 24. 10000 samples were run for the bootstrapped 95% confidence intervals.

Results

Total time spent in the DMN and SN at rest predicted smoking cue reactivity in SN nodes

In two multivariate multiple regression models, we defined DMN (PCC, vmPFC, rACC) or SN (AI and dACC) ROIs as the respective dependent variables. Both models included the total time spent in the DMN or SN state as independent predictors.

In the regression examining DMN nodes, we found that total time spent in both the DMN and SN states did not predict DMN nodal reactivity to smoking cues ($F(6, 82) = 0.89$, $p_{corrected} = 1.00$, $r^2 = 0.12$). In contrast, total time spent in the DMN and SN together significantly predicted SN nodal reactivity to smoking cues ($F(4, 84) = 2.96$, $p_{corrected} = 0.048$, $r^2 = 0.23$, $f^2 = 0.30$). Specifically, time spent in the DMN (Fig. 1A; ß = 0.20, $t = 2.09$, $p = 0.043$, $CI_{95th} = [0.0071, 0.40]$) but not the SN (ß = −0.16, t = −1.22, $p = 0.23$, $CI_{95th} = [-0.42, 0.10]$) positively predicted AI reactivity to smoking cues. In comparison, time spent in the SN (Fig. 1B; ß = −0.44, $t = -2.13$, $p = 0.039$, $CI_{95th} = [-0.85\ -0.024)$ but not the DMN (ß = 0.068, $t = 0.44$, $p = 0.66$, $CI_{95th} = [-0.24, 0.38]$) negatively predicted dACC reactivity to smoking cues.

SN reactivity to smoking cues mediated the relationship between DMN/SN temporal dynamics and changes in subjective craving

Given the regression findings, we explored whether AI and dACC together mediated the relationship between total time spent in either DMN or SN states at rest and changes in craving. Participants' post-cue exposure craving scores were significantly greater than their pre-cue exposure scores ($t(45) = 2.65$, $p = 0.011$). In two mediation models, we respectively defined the DMN or SN resting dynamics as the independent variable. Both models included both AI and dACC as the mediators and changes in craving as the dependent variable.

We found that total time spent in the DMN positively predicted AI reactivity to smoking cues (ß = 0.25, $t = 2.74$, $p = 0.0088$, bootstrapped mean = 0.24, bootstrapped SE = 0.085, $CI_{95thbootstrapped} = [0.074, 0.41]$), AI positively predicted dACC reactivity to smoking cues (ß = 1.02, $t = 5.13$, $p < 0.0001$, bootstrapped mean = 1.02, bootstrapped SE = 0.20, $CI_{95thbootstrapped} = [0.62, 1.42]$), and dACC reactivity to smoking cues positively predicted change in cravings (ß = 0.14, $t = 2.20$, $p = 0.033$, bootstrapped mean = 0.14, bootstrapped SE = 0.061, $CI_{95thbootstrapped} = [0.030, 0.27]$). The overall model of total time in the DMN at rest and AI and dACC reactivity to smoking cues together significantly predicted a cue-induced rise in subjective craving ($F(3, 42) = 3.07$, $p = 0.038$, $r^2 = 0.18$). The only significant indirect effect was yielded by the path from total time in DMN at rest to AI cue reactivity to dACC cue reactivity to changes in craving (Fig. 2A; ß = 0.035, bootstrapped SE = 0.021, $CI_{95thbootstrapped} = [0.0040, 0.085]$), suggesting that AI and dACC together *positively* mediated the relationship between time spent in the DMN and changes in cue-induced craving.

We additionally found that total time spent in SN negatively predicted AI reactivity to smoking cues (ß = −0.26, $t = -2.10$, $p = 0.042$, bootstrapped mean = −0.26, bootstrapped SE = 0.11, $CI_{g5thbootstrapped} = [-0.46, -0.045]$), AI positively predicted dACC reactivity to smoking cues (ß = 0.90, $t = 4.78$, $p < 0.0001$, bootstrapped mean = 0.90, bootstrapped SE =

0.20, $CI_{95thbootstrapped}$ = [0.53, 1.28]), and dACC reactivity to smoking cues positively predicted change in cravings (ß = 0.14, t = 2.15, p = 0.037, bootstrapped mean = 0.15, bootstrapped SE = 0.069, $CI_{95thbootstrapped}$ = [0.022, 0.29]). While the overall model was not significant (F(3, 42) = 1.87, p = 0.15, r^2 = 0.12), there was notably a significant indirect effect for the path from time spent in SN state at rest to AI cue reactivity to dACC cue reactivity to changes in craving (Fig. 2B; ß = −0.033, bootstrapped SE = 0.023, $CI_{95thbootstrapped}$ = [−0.090, −0.0009]), thereby suggesting that AI and dACC together *negatively* mediated the relationship between time spent in the SN and changes in cue-induced craving (35, 36).

Total time spent in the DMN marginally predicted AI subregional reactivity to smoking cues

From aforementioned findings showing that AI cue reactivity was predicted by time spent in the DMN, we conducted a *post-hoc* analysis to study whether this relationship was specific to different AI subregions (37, 38). We ran a multivariate simple regression model with total time in DMN as the independent variable and the four AI subregions as the dependent variables. This model was marginally significant (F(4, 41) = 2.38, p = 0.067, r^2 = 0.19). Specifically, we found that increased time spent in DMN significantly predicted increases in posterior short gyrus (ß = 0.35, t = 3.02, p = 0.004, CI_{95th} = [0.12, 0.58]), anterior short gyrus (ß = 0.23, t = 2.22, p = 0.032, CI_{95th} = [0.021, 0.44]) and anterior pole (ß = 0.21, t = 2.01, p = 0.050, CI_{95th} = [−0.0003, 0.42]) but not middle short gyrus (ß = 0.18, t = 1.57, p = 0.12, CI_{95th} = [−0.050, 0.40]).

AI subregions and dACC reactivity to smoking cues mediated the relationship between DMN resting dynamics and changes in subjective craving

Given our prior significant mediation findings, we conducted *post-hoc* mediation analysis with four AI subregions and dACC as the mediators, total time spent in DMN or SN as the respective independent variable and changes in subjective craving as the dependent variable.

Although no significant *negative* mediation effect was observed for AI subregions on SN dynamics, for DMN dynamics, there was a significant mediation effect observed for posterior short gyrus, middle short gyrus, anterior pole, and dACC. This mediation model (Fig. 3) showed that time spent in the DMN positively predicted posterior short gyrus reactivity to smoking cues (ß = 0.35, t = 3.02, p = 0.0041, bootstrapped mean = 0.35, bootstrapped SE = 0.12, $CI_{95thbootstrapped}$ = [0.11, 0.57]), posterior short gyrus positively predicted middle short gyrus reactivity to smoking cues (ß = 0.59, t = 4.97, p < 0.0001, bootstrapped mean = 0.59, bootstrapped SE = 0.10, $CI_{95thbootstrapped}$ = [0.38, 0.79]), middle short gyrus positively predicted anterior pole reactivity to smoking cues (ß = 0.35, t = 2.33, p = 0.025, bootstrapped mean = 0.35, bootstrapped SE = 0.13, $CI_{95thbootstrapped}$ = [0.093, 0.64]), anterior pole positively predicted dACC reactivity to smoking cues (ß = 0.75, t = 3.85, p = 0.0004, bootstrapped mean = 0.76, bootstrapped SE = 0.16, $CI_{95thbootstrapped}$ = [0.43, 1.07]), and dACC marginally predicted increases in subjective cravings (ß = 0.13, t = 1.90, p = 0.065, bootstrapped mean = 0.13, bootstrapped SE = 0.067, $CI_{95thbootstrapped}$ = [0.010, 0.27]). The overall model was marginally significant (F(5, 40) = 2.33, p = 0.060, r^2 = 0.23) but importantly, there was a significant indirect effect yielded by the path from time spent in DMN at rest to posterior short gyrus to middle short gyrus to anterior pole to dACC

to changes in craving (ß = 0.0069, bootstrapped SE = 0.0054, $CI_{95thbootstrapped}$ = [0.0001, 0.020]), suggesting that AI subregions and dACC together *positively* mediated time spent in the DMN and changes in cue-induced craving (35, 36).

Discussion

We observed that time spent in the DMN and SN states at rest produced opposite predictions on SN reactivity to smoking cues in nicotine-dependent individuals, which fits with the opposing roles of these networks (39). Specifically, *more* time spent in DMN at rest predicted greater AI cue reactivity while *less* time spent in SN at rest predicted greater dACC cue reactivity. Prior work has shown that SUD individuals have hypoconnectivity between DMN nodes at rest (for review see 14) and greater DMN activity during abstinence (18, 40, 41), neural changes that are thought to engender impaired emotion regulation and increased subjective craving (42–44). For SUD individuals, enhanced SN cue reactivity appears to reflect heightened motivated attention towards salient stimuli, triggering greater emotional arousal (45, 46) and cue-induced craving (47, 48). Our findings bridged these two observations by showcasing a predictive relationship between time spent in DMN/SN states at rest and SN cue reactivity, where nicotine-dependent individuals who spent more time in the DMN and less time in the SN were also those who engaged SN neural nodes more strongly when exposed to drug cues. Notably, enhanced AI and dACC cue reactivity have both been linked to relapse vulnerability (4, 9, 10, 49) and thus we infer that resting dynamics of DMN/SN characterize individuals who are more prone to cue reactivity and at greater risk for relapse. As such, resting-state temporal dynamic features such as time spent in state are valuable in serving as a potential biomarker to help predict a core feature of SUD.

The predictive relationship between increased time spent in DMN at rest and cue-induced SN activity is related to the degree in which smoking cues engender increases in subjective craving. Greater DMN static functional connectivity at rest (50, 51) and greater SN neural nodal activity during task (52, 53) have both been connected to heightened cue-induced craving, an observation that is true for nicotine-dependent individuals and those dependent on other substances (40, 54, 55). We built upon this by showing that stronger SN activation to smoking cues mediated the *positive* predictive relationship between time spent in the DMN at rest and cue-induced increases in subjective craving. This mediation effect followed a selective intra-SN pathway from the AI to the dACC, a path which aligns with these regions' respective roles in processing environmentally-salient information (56). According to some models, the AI first assesses the emotional value of the incoming stimuli (57) before transmitting the information to the dACC to plan and initiate future goal-directed actions (58). This AI-dACC path also mediated the relationship between SN resting dynamics and craving changes, albeit in the opposite direction as observed for the DMN, which fits with the opposing roles of the DMN and SN (39). The anatomical heterogeneity of the AI (37, 38) allowed us to further refine this pathway to show that mediation effect followed a posterior-to-anterior trajectory through the AI subregions. This selective pathway recapitulates the functional and anatomical connectivity patterns exhibited by AI subregions, which display an established posterior-to-anterior gradient of information processing (57), and indicates that the more anterior subregions are more connected with frontal cortical

regions including the dACC (59, 60). These findings provide empirical evidence for a specific neurobiological pathway leading to cue-induced subjective craving from resting-state network dynamics.

While our findings have implications for using resting-state networks, particularly that of the DMN, to identify individuals with SUD who are more susceptible to heightened cue reactivity and cue-induced craving, we note that our findings are currently only applicable to nicotine-dependent individuals. We cannot preclude the possibility that chronic nicotine use induces changes that are different from other substances of abuse, potentially narrowing the applicability of the current findings. Future studies are needed to replicate our findings in those with other SUDs. However, given the common neural changes observed in dependent individuals following chronic substance use (61, 62), it seems likely that our findings would be pertinent to other SUD populations. We also did not examine sex, which should be evaluated in future studies. Another potential caveat of the present study is that we applied DMN and SN states from the HCP dataset rather than using data-driven means to establish them in the recruited sample of nicotine-dependent individuals. Although the DMN and SN are well-defined in terms of their anatomical maps, it would be useful for future studies to consider applying the CAPs analysis in a comparatively large sample of nicotine-dependent individuals to clarify the impact of chronic substance use on resting network dynamics. It is also important to include the assessment of other networks such as the executive control network whose involvement in substance dependence is evident (40). However, for this initial analysis relating resting-state dynamics with cue reactivity, a focused analysis of the DMN and SN is supported by the cue-induced activation of these network nodes (7).

In conclusion, our current findings showcased a significant relationship between time spent in the DMN/SN at rest and task-activated nodes of SN that explained the cue-induced rise in subjective craving. Given that increased cue-induced activation of SN nodes predicts relapse vulnerability to tobacco smoking (4, 9, 10, 49), our findings provide insight into the neurobiological processes leading to cue reactivity. Specifically, brain function at rest, prior to cue-exposure, rendered individuals more likely to respond to smoking cues, suggesting that network dynamics influence how the brain responds to externally-salient stimuli. Clinically, this suggests that therapies targeting these network dynamics may mitigate cue reactivity. Present findings also suggest that network dynamics at rest may be a useful biomarker to identify individuals with SUDs who are more susceptible to cue-provoked relapse.

Supplementary Material

Refer to Web version on PubMed Central for supplementary material.

Acknowledgments:

This work was supported by funding from the National Institutes on Drug Abuse K02 DA042987 and R01 DA039135 (ACJ).

Reference

1. Janes AC, Farmer S, Peechatka AL, de B Frederick B, Lukas SE (2015): Insula-dorsal anterior cingulate cortex coupling is associated with enhanced brain reactivity to smoking cues. Neuropsychopharmacology: official publication of the American College of Neuropsychopharmacology. 40:1561–1568. [PubMed: 25567427]
2. Chase HW, Eickhoff SB, Laird AR, Hogarth L (2011): The neural basis of drug stimulus processing and craving: an activation likelihood estimation meta-analysis. Biological psychiatry. 70:785–793. [PubMed: 21757184]
3. Hasin DS, O'Brien CP, Auriacombe M, Borges G, Bucholz K, Budney A, et al. (2013): DSM-5 criteria for substance use disorders: recommendations and rationale. American Journal of Psychiatry. 170:834–851. [PubMed: 23903334]
4. Janes A, Gilman J, Radoman M, Pachas G, Fava M, Evins A (2017): Revisiting the role of the insula and smoking cue-reactivity in relapse: a replication and extension of neuroimaging findings. Drug and alcohol dependence. 179:8–12. [PubMed: 28735078]
5. Weiss F (2005): Neurobiology of craving, conditioned reward and relapse. Current opinion in pharmacology. 5:9–19. [PubMed: 15661620]
6. Courtney KE, Schacht JP, Hutchison K, Roche DJ, Ray LA (2016): Neural substrates of cue reactivity: association with treatment outcomes and relapse. Addiction biology. 21:3–22. [PubMed: 26435524]
7. Engelmann JM, Versace F, Robinson JD, Minnix JA, Lam CY, Cui Y, et al. (2012): Neural substrates of smoking cue reactivity: a meta-analysis of fMRI studies. NeuroImage. 60:252–262. [PubMed: 22206965]
8. Hanlon CA, Hartwell KJ, Canterberry M, Li X, Owens M, LeMatty T, et al. (2013): Reduction of cue-induced craving through realtime neurofeedback in nicotine users: the role of region of interest selection and multiple visits. Psychiatry Research: Neuroimaging. 213:79–81.
9. Allenby C, Falcone M, Wileyto EP, Cao W, Bernardo L, Ashare RL, et al. (2020): Neural cue reactivity during acute abstinence predicts short-term smoking relapse. Addiction biology. 25:e12733. [PubMed: 30806013]
10. Janes AC, Pizzagalli DA, Richardt S, Frederick Bd, Chuzi S, Pachas G, et al. (2010): Brain reactivity to smoking cues prior to smoking cessation predicts ability to maintain tobacco abstinence. Biological psychiatry. 67:722–729. [PubMed: 20172508]
11. Raichle ME (2015): The brain's default mode network. Annual review of neuroscience. 38:433–447.
12. Menon V, Uddin LQ (2010): Saliency, switching, attention and control: a network model of insula function. Brain Structure and Function. 214:655–667. [PubMed: 20512370]
13. Barrett LF, Satpute AB (2013): Large-scale brain networks in affective and social neuroscience: towards an integrative functional architecture of the brain. Current opinion in neurobiology. 23:361–372. [PubMed: 23352202]
14. Zhang R, Volkow ND (2019): Brain default-mode network dysfunction in addiction. NeuroImage. 200:313–331. [PubMed: 31229660]
15. Biswal B, Zerrin Yetkin F, Haughton VM, Hyde JS (1995): Functional connectivity in the motor cortex of resting human brain using echo-planar MRI. Magnetic resonance in medicine. 34:537–541. [PubMed: 8524021]
16. Fedota JR, Stein EA (2015): Resting-state functional connectivity and nicotine addiction: prospects for biomarker development. Annals of the New York Academy of Sciences. 1349:64. [PubMed: 26348486]
17. Hsu L-M, Keeley RJ, Liang X, Brynildsen JK, Lu H, Yang Y, et al. (2019): Intrinsic insular-frontal networks predict future nicotine dependence severity. Journal of Neuroscience. 39:5028–5037. [PubMed: 30992371]
18. Lerman C, Gu H, Loughead J, Ruparel K, Yang Y, Stein EA (2014): Large-scale brain network coupling predicts acute nicotine abstinence effects on craving and cognitive function. JAMA psychiatry. 71:523–530. [PubMed: 24622915]

19. Hutchison RM, Womelsdorf T, Allen EA, Bandettini PA, Calhoun VD, Corbetta M, et al. (2013): Dynamic functional connectivity: promise, issues, and interpretations. NeuroImage. 80:360–378. [PubMed: 23707587]
20. Fedota JR, Ding X, Matous AL, Salmeron BJ, McKenna MR, Gu H, et al. (2018): Nicotine abstinence influences the calculation of salience in discrete insular circuits. Biological Psychiatry: Cognitive Neuroscience and Neuroimaging. 3:150–159. [PubMed: 29529410]
21. Janes AC, Peechatka AL, Frederick BB, Kaiser RH (2020): Dynamic functioning of transient resting-state coactivation networks in the Human Connectome Project. Human brain mapping. 41:373–387. [PubMed: 31639271]
22. Janes AC, Krantz NL, Nickerson LD, Frederick BB, Lukas SE (2020): Craving and Cue Reactivity in Nicotine-Dependent Tobacco Smokers Is Associated With Different Insula Networks. Biological Psychiatry: Cognitive Neuroscience and Neuroimaging. 5:76–83. [PubMed: 31706906]
23. Fagerstrom K-O (1978): Measuring degree of physical dependence to tobacco smoking with reference to individualization of treatment. Addictive behaviors. 3:235–241. [PubMed: 735910]
24. First MB, Spitzer RL, Gibbon M, Williams JB (2002): Structured clinical interview for DSM-IV-TR axis I disorders, research version, patient edition. SCID-I/P New York, NY.
25. Cox LS, Tiffany ST, Christen AG (2001): Evaluation of the brief questionnaire of smoking urges (QSU-brief) in laboratory and clinical settings. Nicotine & Tobacco Research. 3:7–16. [PubMed: 11260806]
26. Griffanti L, Douaud G, Bijsterbosch J, Evangelisti S, Alfaro-Almagro F, Glasser MF, et al. (2017): Hand classification of fMRI ICA noise components. NeuroImage. 154:188–205. [PubMed: 27989777]
27. Kelly RE Jr, Alexopoulos GS, Wang Z, Gunning FM, Murphy CF, Morimoto SS, et al. (2010): Visual inspection of independent components: defining a procedure for artifact removal from fMRI data. Journal of neuroscience methods. 189:233–245. [PubMed: 20381530]
28. Andrews-Hanna JR, Reidler JS, Sepulcre J, Poulin R, Buckner RL (2010): Functional-anatomic fractionation of the brain's default network. Neuron. 65:550–562. [PubMed: 20188659]
29. Seeley WW, Menon V, Schatzberg AF, Keller J, Glover GH, Kenna H, et al. (2007): Dissociable intrinsic connectivity networks for salience processing and executive control. Journal of Neuroscience. 27:2349–2356. [PubMed: 17329432]
30. Janes AC, Nickerson LD, Frederick Bd, Kaufman MJ (2012): Prefrontal and limbic resting state brain network functional connectivity differs between nicotine-dependent smokers and non-smoking controls. Drug and alcohol dependence. 125:252–259. [PubMed: 22459914]
31. Desikan RS, Segonne F, Fischl B, Quinn BT, Dickerson BC, Blacker D, et al. (2006): An automated labeling system for subdividing the human cerebral cortex on MRI scans into gyral based regions of interest. NeuroImage. 31:968–980. [PubMed: 16530430]
32. Janes AC, Zegel M, Ohashi K, Betts J, Molokotos E, Olson D, et al. (2018): Nicotine normalizes cortico-striatal connectivity in non-smoking individuals with major depressive disorder. Neuropsychopharmacology: official publication of the American College of Neuropsychopharmacology. 43:2445–2451. [PubMed: 29795403]
33. Faillenot I, Heckemann RA, Frot M, Hammers A (2017): Macroanatomy and 3D probabilistic atlas of the human insula. NeuroImage. 150:88–98. [PubMed: 28179166]
34. Hayes AF (2012): PROCESS: A versatile computational tool for observed variable mediation, moderation, and conditional process modeling. University of Kansas, KS.
35. Zhao X, Lynch JG Jr, Chen Q (2010): Reconsidering Baron and Kenny: Myths and truths about mediation analysis. Journal of consumer research. 37:197–206.
36. Agler R, De Boeck P (2017): On the interpretation and use of mediation: multiple perspectives on mediation analysis. Frontiers in psychology. 8:1984. [PubMed: 29187828]
37. Uddin LQ, Nomi JS, Hebert-Seropian B, Ghaziri J, Boucher O (2017): Structure and function of the human insula. Journal of clinical neurophysiology: official publication of the American Electroencephalographic Society. 34:300. [PubMed: 28644199]
38. Wager TD, Barrett LF (2017): From affect to control: Functional specialization of the insula in motivation and regulation. BioRxiv.102368.

39. Menon V (2015): Salience network In: Toga AW, editor. Brain Mapping: An Encyclopedic Reference: Academic Press: Elsevier, pp 597–611.
40. Sutherland MT, McHugh MJ, Pariyadath V, Stein EA (2012): Resting state functional connectivity in addiction: lessons learned and a road ahead. NeuroImage. 62:2281–2295. [PubMed: 22326834]
41. Hahn B, Ross TJ, Yang Y, Kim I, Huestis MA, Stein EA (2007): Nicotine enhances visuospatial attention by deactivating areas of the resting brain default network. Journal of Neuroscience. 27:3477–3489. [PubMed: 17392464]
42. Li Q, Li Z, Li W, Zhang Y, Wang Y, Zhu J, et al. (2016): Disrupted Default Mode Network and Basal Craving in Male Heroin-Dependent Individuals: A Resting-State fMRI Study. The Journal of clinical psychiatry. 77:e1211–e1217. [PubMed: 27574841]
43. Li W, Li Q, Wang D, Xiao W, Liu K, Shi L, et al. (2015): Dysfunctional default mode network in methadone treated patients who have a higher heroin relapse risk. Scientific reports. 5:1–8.
44. Carhart-Harris RL, Erritzoe D, Williams T, Stone JM, Reed LJ, Colasanti A, et al. (2012): Neural correlates of the psychedelic state as determined by fMRI studies with psilocybin. Proceedings of the National Academy of Sciences. 109:2138–2143.
45. Luijten M, Veltman DJ, van den Brink W, Hester R, Field M, Smits M, et al. (2011): Neurobiological substrate of smoking-related attentional bias. NeuroImage. 54:2374–2381. [PubMed: 20932921]
46. Noori HR, Linan AC, Spanagel R (2016): Largely overlapping neuronal substrates of reactivity to drug, gambling, food and sexual cues: A comprehensive meta-analysis. European Neuropsychopharmacology. 26:1419–1430. [PubMed: 27397863]
47. Kühn S, Gallinat J (2011): Common biology of craving across legal and illegal drugs-a quantitative meta-analysis of cue-reactivity brain response. European Journal of Neuroscience. 33:1318–1326. [PubMed: 21261758]
48. Scott D, Hiroi N (2011): Deconstructing craving: dissociable cortical control of cue reactivity in nicotine addiction. Biological psychiatry. 69:1052–1059. [PubMed: 21429478]
49. Sinha R (2011): New findings on biological factors predicting addiction relapse vulnerability. Current psychiatry reports. 13:398. [PubMed: 21792580]
50. Wang Z, Faith M, Patterson F, Tang K, Kerrin K, Wileyto EP, et al. (2007): Neural substrates of abstinence-induced cigarette cravings in chronic smokers. Journal of Neuroscience. 27:14035–14040. [PubMed: 18094242]
51. Li Y, Yuan K, Bi Y, Guan Y, Cheng J, Zhang Y, et al. (2017): Neural correlates of 12-h abstinence-induced craving in young adult smokers: a resting-state study. Brain imaging and behavior. 11:677–684. [PubMed: 26995747]
52. Tang D, Fellows L, Small D, Dagher A (2012): Food and drug cues activate similar brain regions: a meta-analysis of functional MRI studies. Physiology & behavior. 106:317–324. [PubMed: 22450260]
53. Brody AL, Mandelkern MA, London ED, Childress AR, Lee GS, Bota RG, et al. (2002): Brain metabolic changes during cigarette craving. Archives of general psychiatry. 59:1162–1172. [PubMed: 12470133]
54. Limbrick-Oldfield EH, Mick I, Cocks R, McGonigle J, Sharman S, Goldstone AP, et al. (2017): Neural substrates of cue reactivity and craving in gambling disorder. Translational psychiatry. 7:e992–e992. [PubMed: 28045460]
55. Bonson KR, Grant SJ, Contoreggi CS, Links JM, Metcalfe J, Weyl HL, et al. (2002): Neural systems and cue-induced cocaine craving. Neuropsychopharmacology: official publication of the American College of Neuropsychopharmacology. 26:376–386. [PubMed: 11850152]
56. Lamichhane B, Dhamala M (2015): The salience network and its functional architecture in a perceptual decision: an effective connectivity study. Brain connectivity. 5:362–370. [PubMed: 25578366]
57. Craig AD, Craig A (2009): How do you feel--now? The anterior insula and human awareness. Nature reviews neuroscience. 10.
58. Holroyd CB, Yeung N (2012): Motivation of extended behaviors by anterior cingulate cortex. Trends in cognitive sciences. 16:122–128. [PubMed: 22226543]

59. Deen B, Pitskel NB, Pelphrey KA (2011): Three systems of insular functional connectivity identified with cluster analysis. Cerebral cortex. 21:1498–1506. [PubMed: 21097516]

60. Medford N, Critchley HD (2010): Conjoint activity of anterior insular and anterior cingulate cortex: awareness and response. Brain Structure and Function. 214:535–549. [PubMed: 20512367]

61. Trigo JM, Martin-Garcia E, Berrendero F, Robledo P, Maldonado R (2010): The endogenous opioid system: a common substrate in drug addiction. Drug and alcohol dependence. 108:183–194. [PubMed: 19945803]

62. Nestler EJ (2005): Is there a common molecular pathway for addiction? Nature neuroscience. 8:1445–1449. [PubMed: 16251986]

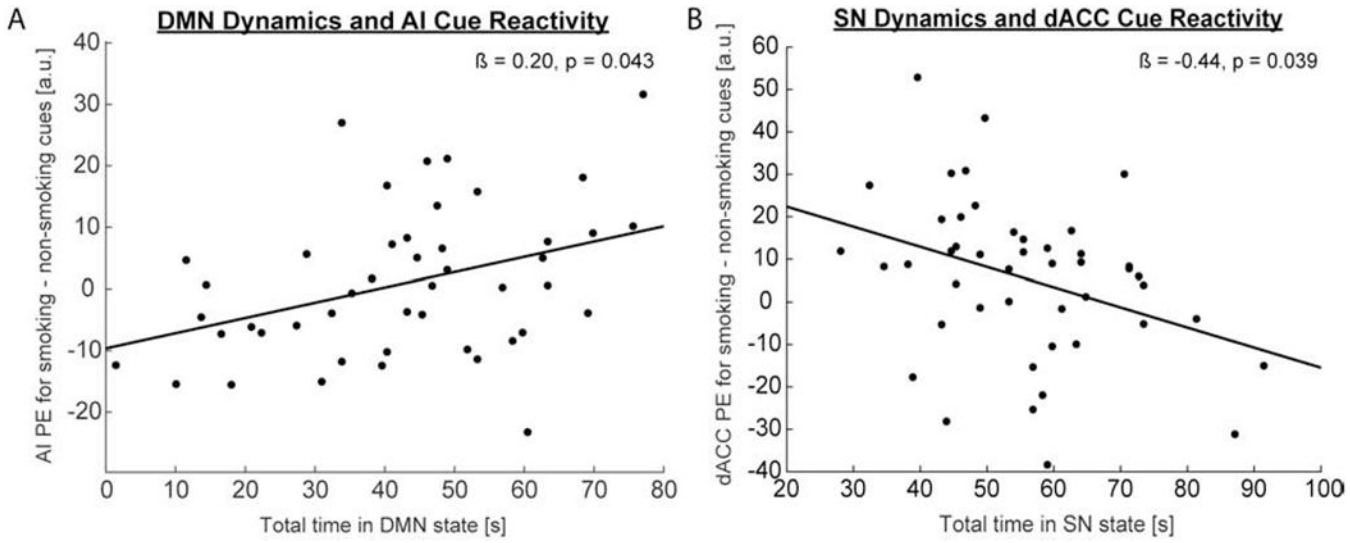

Fig. 1. Network dynamics predict smoking cue reactivity in SN nodes.

(A). Increased total time spent (in seconds) in the DMN at rest significantly predicted increased AI reactivity (labeled as PE = parameter estimate with arbitrary units [a.u.] in figure) to smoking cues during task. **(B).** Decreased total time spent in the SN at rest significantly predicted increased dACC reactivity to smoking cues during task.

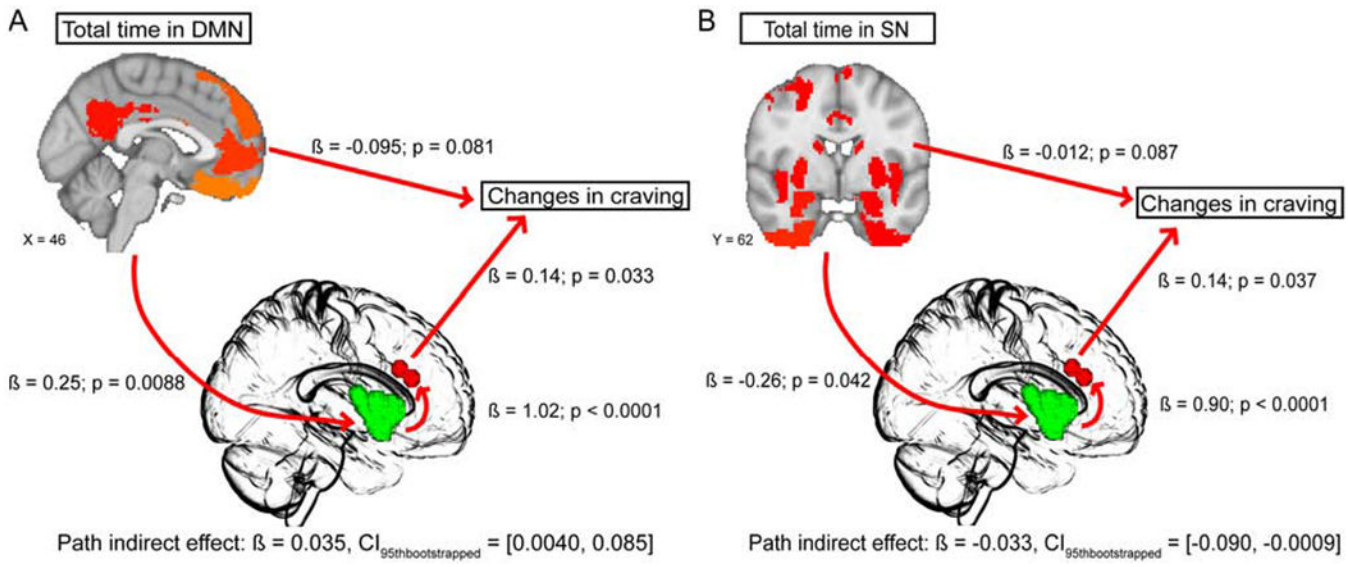

Fig. 2. Mediation model of DMN/SN dynamics at rest and changes in cue-induced subjective craving.

We applied mediation models where neural cue reactivities were the mediators for the relationship between either DMN or SN resting dynamics and changes in craving. **A.** In the model examining DMN dynamics, the path from total time spent in DMN at rest to AI (green in center brain template) cue reactivity to dACC (red in center brain template) cue reactivity to changes in craving yielded a significant indirect mediation effect, suggesting that AI and dACC together positively mediated the relationship between DMN resting dynamics and cue-induced craving. **B.** In the model examining SN dynamics, the path from total time spent in SN at rest to AI (green in center brain template) cue reactivity to dACC (red in center brain template) cue reactivity to changes in craving produced a significant indirect mediation effect, suggesting that AI and dACC significantly negatively mediated the relationship between SN resting dynamics and subjective cue-induced craving.

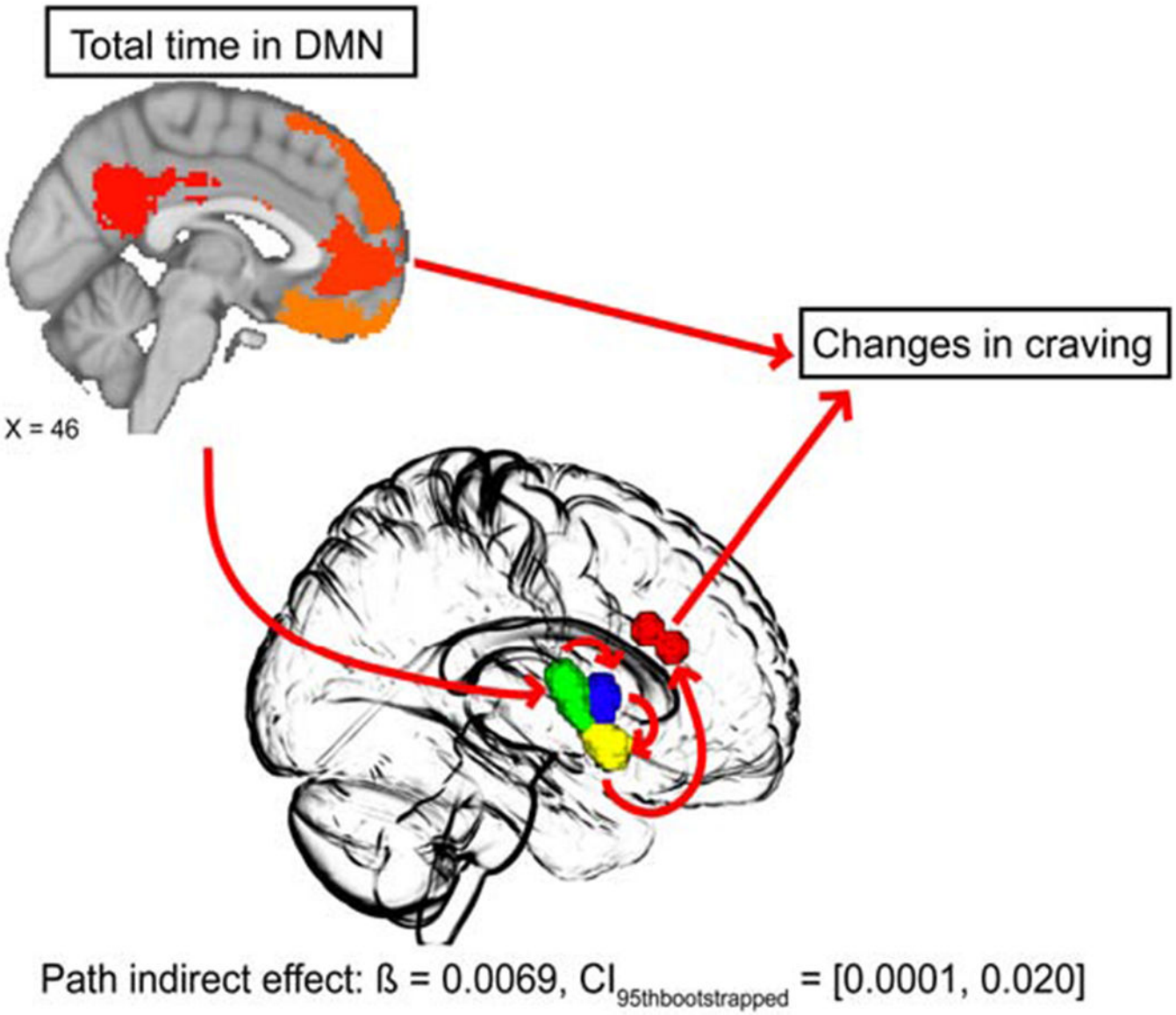

Fig. 3. Mediation model using AI subregions as mediators.

We applied a model where neural cue reactivity of AI subregions and dACC were the mediators and found that posterior short gyrus (green in center brain template), middle short gyrus (blue in center brain template), anterior pole (yellow in center brain template) and dACC (red in center brain template) together significantly positively mediated the relationship between time spent in the DMN state at rest and cue-induced subjective craving. Specifically, the path, beginning with total time in the DMN state to posterior short gyrus cue reactivity, to middle short gyrus cue reactivity, to anterior pole cue reactivity, to dACC cue reactivity, and ultimately to changes in cravings yielded a significant indirect effect.

Table 1.

Participants' characteristics.

Characteristics	Means (SD)
Age, Years	29.48 (6.48)
Education, Years	15.11 (1.76)
Fagerström Test for Nicotine Dependence Score	5.59 (1.59)
Average Number of Cigarettes per Day	13.67 (5.52)
Pack-years	8.61 (1.76)
Age Started Smoking, Years	17.58 (3.98)
QSU Pre-cue exposure	18.72 (1.13)
QSU Post-cue exposure	21.26 (1.39)